



Bellcomm

955 L'Enfant Plaza North, S.W.
Washington, D. C. 20024

B71 09029

date: September 30, 1971
to: Distribution
from: T. J. Rudd
subject: A Hydroelastic Model for a Cylindrical
Tank with an Inverted Bulkhead - Case 320

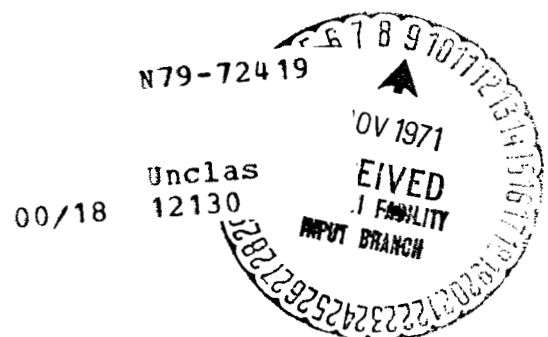
ABSTRACT

The POGO study of large liquid fueled rockets, such as the Saturn V, requires an accurate structural model. In particular, the axial motion of the liquid propellant must be accurately represented. There are in existence hydroelastic models that may be used to represent liquid propellants which are contained in ellipsoidal type tanks such as the Saturn S-IVB or S-II liquid oxygen tanks. However, no corresponding hydroelastic model exists for representing the liquid hydrogen of these stages, where the containing tanks are cylindrical but with inverted bulkheads.

As part of an effort to obtain a more detailed structural model of the S-IVB, a hydroelastic model for the liquid hydrogen was developed and is described in this memorandum.

A computer program for finding the corresponding liquid mass matrix is briefly described, and a sample problem solved using this program. Two theoretical checks on the computed mass matrix are made and it is shown that the accuracy of the numerical procedure is very good.

(NASA-CR-123237) A HYDROELASTIC MODEL FOR A
CYLINDRICAL TANK WITH AN INVERTED BULKHEAD
(Bellcomm, Inc.) 30 p



FF No. 78-123237 (NASA CR OR TMX OR AD NUMBER) (CATEGORY)
AVAILABLE TO NASA OFFICES AND NASA
RESEARCH CENTERS ONLY



Bellcomm

955 L'Enfant Plaza North, S.W.
Washington, D. C. 20024

date: September 30, 1971
to: Distribution
from: T. J. Rudd
subject: A Hydroelastic Model for a Cylindrical
Tank with an Inverted Bulkhead - Case 320

B71 09029

MEMORANDUM FOR FILE

1. INTRODUCTION

In the POGO study of large liquid fueled space vehicles, such as the Saturn V, it has been understood for some time that an accurate structural model of the vehicle is required. For this an accurate representation of the axial motion of the liquid propellant, must be found. Furthermore, it must be of a type that can be easily incorporated into an overall structural model of the vehicle.

To this end a number of hydroelastic models have been developed [1, 2]. Using such a model for the liquid (LOX) most of the observed Saturn V POGO instabilities have been successfully predicted by closed loop analysis. There are, however, some time points, notably during the S-IVB first burn, at which inflight vibrations have been observed but for which the analysis has predicted a large degree of stability. This suggests that the structural model may need refinement and in particular that a hydroelastic representation be used for the liquid hydrogen (LH₂) as well as the LOX.

Previously the LH₂ has not received such careful modelling as the LOX for several reasons. One reason is that due to the stiff nature of the LH₂ tank lower bulkhead and the relatively small mass of the LH₂, it was thought that any vibrational activity of the LH₂ would be in a frequency range above that of POGO. Another reason is that in POGO analysis the LH₂ tank bottom pressure fluctuation, unlike the LOX, has little influence on the engine thrust fluctuation. (For an accurate determination this requires a hydroelastic model [3].) Finally none of the existing hydroelastic models



are suitable for a liquid contained in a cylindrical tank with an inverted lower bulkhead such as the S-IVB or SII LH₂ tanks.

In this memorandum a hydroelastic model is derived for a liquid contained in an elastic cylindrical tank whose lower bulkhead is an inverted partial ellipsoid. The analysis is based on the finite difference technique of Goldman [2] but uses the variable mesh version of the finite difference grid as detailed by Vandergraft [4]. A computer program, which can be used to compute the corresponding mass matrix for the liquid is described and an example problem solved using this program. The accuracy of the method is checked.

2. PROBLEM AND SYSTEM DEFINITION

The problem considered here is to find a liquid mass matrix for the system whose cross section is shown in Figure 1. The tank consists of a cylindrical portion, which, in general, is capped at both ends by partial ellipsoids. The lower end is made up of two ellipsoids; one is inverted and has center O1 while the other is regular with center at O2. The upper end of the tank is capped by a semi-ellipsoid with center at O4.

The tank shown in Figure 1 has the same geometry as the S-IVB LH₂ tank and as such is the most complicated of the LH₂ tanks in the Saturn V vehicle. Consequently an analysis carried out for this tank may be easily applied to the fuel tank of the S-IC or the LH₂ tank of the S-II stage. In both of these tanks the lower end is closed out by a single semi-ellipsoid (in the S-II stage it is inverted while in the S-IC stage it is regular).

The liquid is assumed to be incompressible and inviscid, these being valid assumptions for the liquid propellants to be studied. The free surface of the liquid is assumed to be anywhere between the lowest point, defined by the intersection of S1 and S2, (see Figure 1), and the highest point of the tank. The space between the free surface and the top of the tank is occupied by ullage gas whose dynamics will be ignored here.

The mass matrix for the liquid depends on the degrees-of-freedom chosen to represent its motion. It may be easily shown (see Section 3) that the motion of the fluid is completely determined once the motion of its boundary is known. Hence the degrees-of-freedom for the liquid can be chosen to be those used to represent the tank structure (with the exception of the liquid free surface).[†] These degrees-of-freedom are the

[†] see note on page 6.

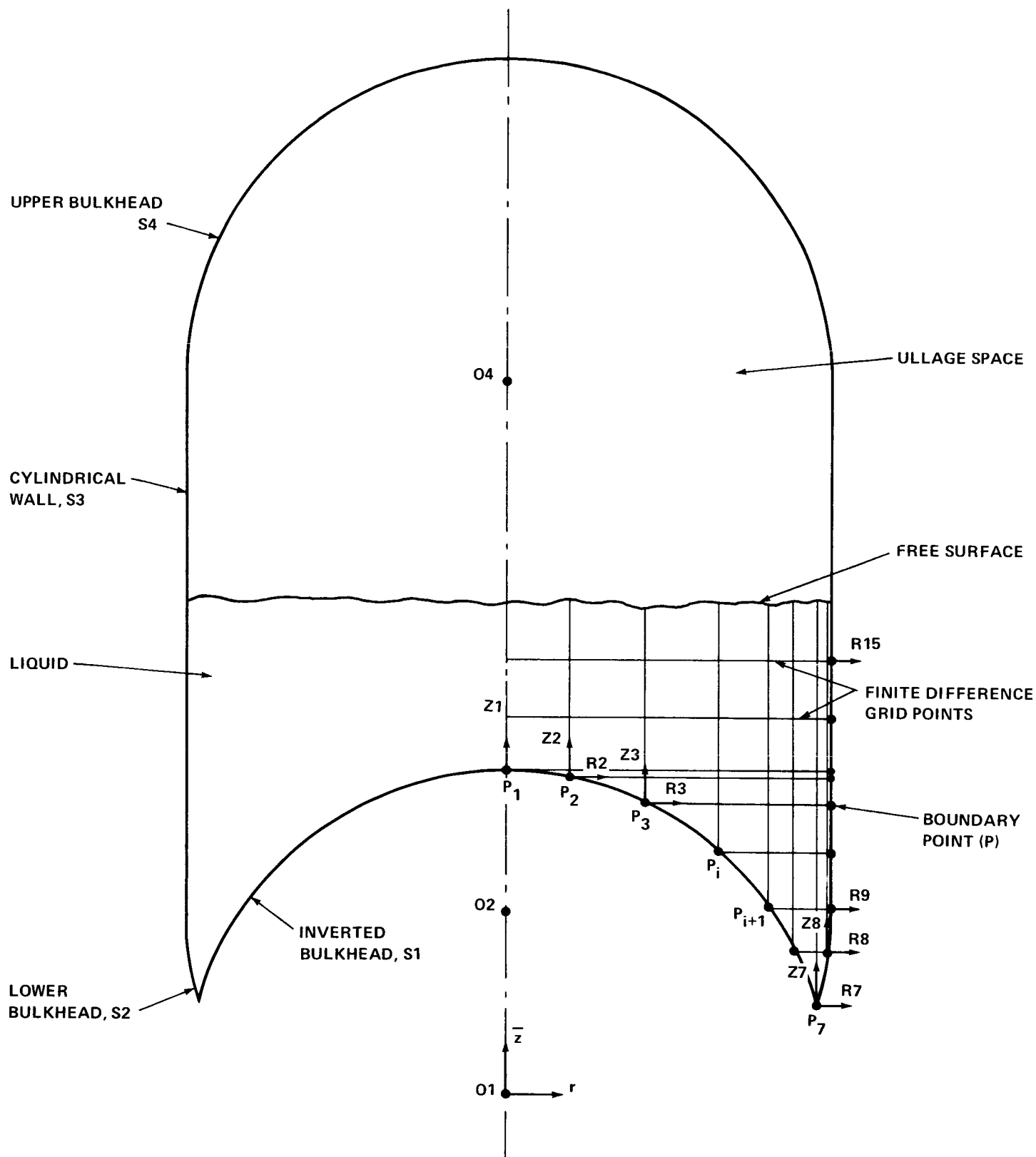


FIGURE 1 - AXISYMMETRIC CYLINDRICAL TANK SYSTEM SHOWING FINITE DIFFERENCE GRID, BOUNDARY POINTS AND ASSOCIATED DEGREES OF FREEDOM



vertical (Z) and radial (R) displacements of the boundary points (P), as shown in Figure 1. While these points will be chosen to make the stiffness matrix calculation for the tank as simple as possible, for the finite difference solution they must be chosen such that

- (i) corresponding points on bulkhead S1 and S2 are in the same horizontal level,
- (ii) corresponding points on bulkhead S2 (or S1) and S4 lie on the same vertical lines. (See Figure 1.)

3. DERIVATION OF THE LIQUID MASS MATRIX

In view of the connection between mass and kinetic energy for a liquid, once a discrete form of the kinetic energy is known the mass matrix can be easily found. The procedure for finding the mass matrix is based, then, on first finding the kinetic energy of the liquid in terms of a finite number of normal velocities of the tank wall.

The kinetic energy of the liquid is

$$T = \frac{\rho}{2} \int_V \underline{v} \cdot \underline{v} dV , \quad (1)$$

where ρ is the liquid mass density, $\underline{v} = \underline{v}(r, z, t)$ is the axisymmetric velocity field, and the integration is carried out over the volume V occupied by the liquid.

From the assumption that the liquid is incompressible we find from the continuity equation

$$\text{div } \underline{v} = 0 . \quad (2)$$

Furthermore for an inviscid liquid, which is at rest initially, we may assume the resulting motion is irrotational, i.e., there exists a potential function $\phi = \phi(r, z, t)$ such that



$$\underline{v} = \nabla \phi \quad . \quad (3)$$

Combining (2) and (3) we find

$$\nabla^2 \phi = 0 \quad . \quad (4)$$

Applying Green's first identity to the integral in (1) and using (3) and (4) we find the equivalent expression for the kinetic energy

$$T = \frac{\rho}{2} \int_{S_T} \phi \frac{\partial \phi}{\partial n} dS \quad , \quad (5)$$

where $\frac{\partial \phi}{\partial n}$ is the derivative of ϕ in the direction of the outward normal to the liquid surface. The integration is extended over the total bounding surface, S_T , of the liquid, which includes both the free surface area, S_F , and the wetted area of the tank, S_S .

Now on the free surface the pressure of the liquid equals the ullage pressure (which will be assumed constant) and hence the linearized Bernoulli equation can be taken in the form

$$\frac{\partial \phi}{\partial t} + a_z \eta = 0 \quad . \quad (6)$$

Here a_z is the inertial acceleration of the tank relative to the local gravitational acceleration, $\eta(r,t)$ is the instantaneous free surface wave height, and $\frac{\partial \phi}{\partial t}(r,t)$ is the velocity potential rate at the free surface.



Goldman [2] has observed that for hydroelastic vibrations of tanks in rockets, which are accelerating at moderate g levels ($\leq 5g$), to a good approximation ϕ satisfies the equation

$$\frac{\partial \phi}{\partial t} = 0 \quad , \quad (7)$$

on the free surface. For vibratory motion this is equivalent to

$$\phi = 0 \quad . \quad (8)$$

Using (8) in (5) we therefore find for the kinetic energy the simpler expression,

$$T = \frac{\rho}{2} \int_{S_S} \phi \frac{\partial \phi}{\partial n} dS \quad , \quad (9)$$

where now the integration is only taken over the wetted area, S_S of the tank.

Now the integral in (9) can be evaluated by using the values of the integrand at N discrete points as

$$T = \frac{\rho}{2} \sum_{i,j=1}^N \phi_i \bar{G}_{ij} \left(\frac{\partial \phi}{\partial n} \right)_j \quad , \quad (10)$$

where ϕ_i is the value of the potential at the i th point, $\left(\frac{\partial \phi}{\partial n} \right)_j$ is the normal velocity of the liquid boundary at the j th point, and \bar{G}_{ij} is a banded integration matrix. The elements of this matrix may be found from (9) by assuming the potential function and normal velocity to vary linearly with arc length between



two consecutive points P_i and P_{i+1} (see Figure 1). (For more details of the calculation of the \bar{G} matrix see Reference [3].) Since the liquid is inviscid, the compatibility condition between the liquid and tank is

$$v_j = \left(\frac{\partial \phi}{\partial n} \right)_j \quad (j = 1, N) , \quad (11)$$

where v_j is the normal velocity of the tank at the j th point.

From a finite difference solution of (4) subject to the boundary conditions (8) and (11) we can find a relationship of the form

$$\phi_i = \sum_{j=1}^N Q_{ij} v_j , \quad (12)$$

with Q_{ij} a known matrix.

Substituting for $\left(\frac{\partial \phi}{\partial n} \right)_j$ and ϕ_i in (10) gives the required discrete form for the kinetic energy

$$T = \frac{\rho}{2} \sum_{i,j,k=1}^N v_k Q_{ki} \bar{G}_{ij} v_j . \quad (13)$$

Finally the liquid mass matrix can be found by noting from Lagrange's equation (the governing equations for the motion) that the inertial properties are contained in the terms

$\frac{d}{dt} \left(\frac{\partial T}{\partial v_\ell} \right)$, where v_ℓ ($\ell = 1, N$) are the generalized velocities.



Using (13) we find,

$$\begin{aligned} \frac{d}{dt} \left(\frac{\partial T}{\partial \dot{v}_\ell} \right) &= \frac{\rho}{2} \left\{ \sum_{i,j,k=1}^N \delta_{kl} Q_{ki} \bar{G}_{ij} \dot{v}_j + \sum_{i,j,k=1}^N \dot{v}_k Q_{ki} \bar{G}_{ij} \delta_{j\ell} \right\} \quad (\ell=1,N) \\ &= \frac{\rho}{2} \sum_{i,k=1}^N (Q_{k\ell} \bar{G}_{ik} + Q_{ki} \bar{G}_{i\ell}) \dot{v}_k \quad (\ell=1,N) . \end{aligned} \quad (14)$$

Hence in matrix notation the liquid mass matrix, M is given by

$$M = \frac{\rho}{2} [\bar{G}Q + (\bar{G}Q)^T] . \quad (15)$$

4. FINITE DIFFERENCE SOLUTION

The central problem in the derivation of the hydroelastic model by finite differences is the derivation of the Q_{ij} matrix. As indicated, this is found by constructing a solution for Laplace's equation (4) subject to the boundary conditions (8) and (11). Since the motion is assumed axisymmetric we need only consider the solution of ϕ in the quarter section shown in Figure 1. From the assigned boundary points the grid is constructed as shown in Figure 1. As previously noted, the boundary points may be chosen at random so long as they can be joined by vertical and horizontal grid lines and there are grid points at the joins of the sections S1 and S2, S2 and S3, etc.

In cylindrical coordinates, Laplace's equation (4) has the form

$$\frac{1}{r} \frac{\partial \phi}{\partial r} + \frac{\partial^2 \phi}{\partial r^2} + \frac{\partial^2 \phi}{\partial z^2} = 0 . \quad (16)$$

For convenience we introduce the non-dimensional variables $\lambda = r/R$ and $z = \bar{z}/R$, where R is the maximum radius of the tank. In non-dimensional form (16) becomes



$$\frac{1}{\lambda} \frac{\partial \tilde{\phi}}{\partial \lambda} + \frac{\partial^2 \tilde{\phi}}{\partial \lambda^2} + \frac{\partial^2 \tilde{\phi}}{\partial z^2} = 0 , \quad (17)$$

where $\phi(\lambda, z) = \phi(r(\lambda), \bar{z}(z))$ for all λ and z .

Approximating the terms in (17) by central differences we find for the general interior point (i, j) , Figure 2, the equation

$$\begin{aligned} & \frac{-1}{(\alpha_j + \alpha_{j-1})} \left\{ \frac{1}{\alpha_{j-1}} - \frac{1}{2\lambda_j} \right\} \tilde{\phi}_{i,j-1} + \frac{-1}{\beta_{i-1}(\beta_{i-1} + \beta_i)} \tilde{\phi}_{i-1,j} \\ & + \frac{-1}{\beta_i(\beta_{i-1} + \beta_i)} \tilde{\phi}_{i+1,j} + \frac{-1}{(\alpha_j + \alpha_{j-1})} \left\{ \frac{1}{\alpha_j} + \frac{1}{2\lambda_j} \right\} \tilde{\phi}_{i,j+1} \\ & + \left(\frac{1}{\alpha_j \alpha_{j-1}} + \frac{1}{\beta_i \beta_{i-1}} \right) \tilde{\phi}_{i,j} = 0 , \end{aligned} \quad (18)$$

where $\tilde{\phi}_{i,j}$ is the approximation to $\tilde{\phi}$ at the point (i, j) , $\tilde{\phi}_{i-1,j}$ is the approximation to $\tilde{\phi}$ at $(i-1, j)$, and so on.

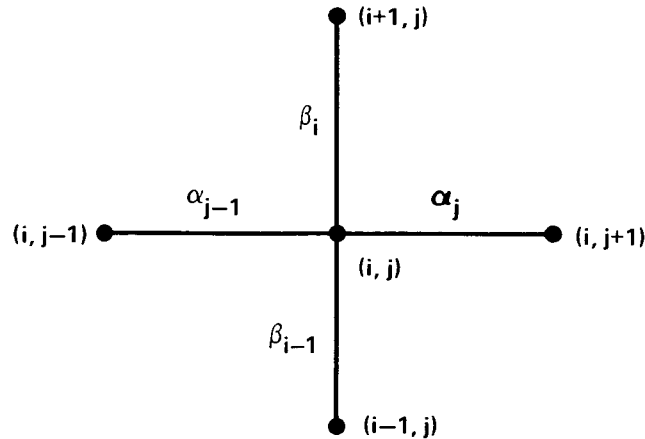


FIGURE 2 - GENERAL INTERIOR POINT



For points on the axis we note that Laplace's equation has the form

$$\frac{2\partial^2 \tilde{\phi}}{2\lambda^2} + \frac{\partial^2 \tilde{\phi}}{\partial z^2} = 0 . \quad (19)$$

The corresponding finite difference approximation is

$$\begin{aligned} \frac{-2}{\alpha_j^2} \tilde{\phi}_{i,j+1} + \frac{-1}{\beta_{i-1}(\beta_{i-1} + \beta_i)} \tilde{\phi}_{i-1,j} + \frac{-1}{\beta_i(\beta_{i-1} + \beta_i)} \tilde{\phi}_{i+1,j} \\ + \left(\frac{2}{\alpha_j^2} + \frac{1}{\beta_i \beta_{i-1}} \right) \tilde{\phi}_{i,j} = 0 . \end{aligned} \quad (20)$$

To complete the finite difference solution we must add equations for the boundary points. Since the potential at the free surface is zero we need only write equations for the boundary points in contact with the tank wall. At these points (taking account of the normalization)

$$\left(\frac{\partial \tilde{\phi}}{\partial n} \right)_i = Rv_i \quad (i=1, N) , \quad (21)$$

where as previously stated v_i is the normal velocity of the tank at the point i . The next step is to suitably express $\left(\frac{\partial \tilde{\phi}}{\partial n} \right)_i$ in terms of the potential at the boundary and interior points. Here a first order approximation to the derivative $\left(\frac{\partial \tilde{\phi}}{\partial n} \right)_i$ is sufficient since the approximations to the interior points are only to this order [4]. Since the expression for $\left(\frac{\partial \tilde{\phi}}{\partial n} \right)_i$ varies with the geometry of the tank the equations for the boundary points on S1, S2, S3 and S4 must be considered separately. Furthermore, the corner point at the discontinuous intersection of S1 and S2 needs special consideration.



Boundary Point on S1

The normal at the point P_0 makes an angle of Ω_0 with the horizontal. The mesh points adjacent to P_0 in the horizontal and vertical directions are P_1 and P_2 , respectively (see Figure 3).

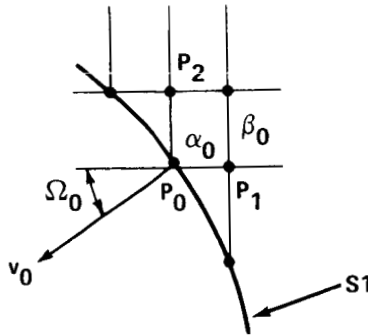


FIGURE 3 - BOUNDARY POINT ON S1

Now resolving along the normal gives

$$\left(\frac{\partial \tilde{\phi}}{\partial n}\right)_{P_0} = -\left(\frac{\partial \tilde{\phi}}{\partial \lambda}\right)_{P_0} \cos \Omega_0 - \left(\frac{\partial \tilde{\phi}}{\partial z}\right)_{P_0} \sin \Omega_0. \quad (22)$$

Using the first order approximations

$$\left. \begin{aligned} \left(\frac{\partial \tilde{\phi}}{\partial \lambda}\right)_{P_0} &= \frac{\tilde{\phi}(P_1) - \tilde{\phi}(P_0)}{\alpha_0} \\ \left(\frac{\partial \tilde{\phi}}{\partial z}\right)_{P_0} &= \frac{\tilde{\phi}(P_2) - \tilde{\phi}(P_1)}{\beta_0} \end{aligned} \right\} \quad (23)$$



we find the equation for the boundary point on S1 to be

$$\frac{\cos \Omega_0}{\alpha_0} \tilde{\phi}(P_0) - \frac{\sin \Omega_0}{\beta_0} \tilde{\phi}(P_2) + \left(\frac{\sin W_0}{\beta_0} - \frac{\cos W_0}{\alpha_0} \right) \tilde{\phi}(P_1) = R v_0 \quad (24)$$

Boundary Points on S2, S3 and S4

The equations for these boundary points can be derived in the same way as those for the surface S. The exact form of these equations is given in Appendix A.

Corner Point at the Intersection of S1 and S2

To facilitate the numerical integration of the kinetic energy expression, (9), in the neighborhood of P_0 (see Figure 4) we identify two normals: one associated with the direction of V_0 , which is perpendicular to the surface S1 and makes an angle of Ω_0 with the horizontal; the other associated with the direction of V_{0s} , which is perpendicular to the surface S2 and makes an angle of Ω_{0s} with the horizontal.

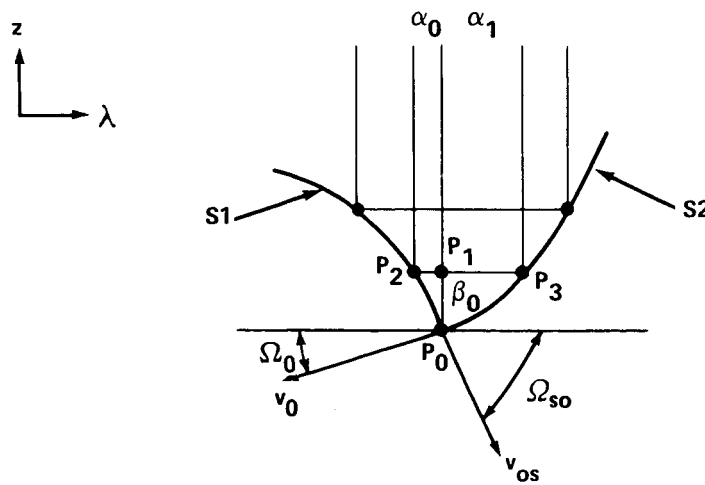


FIGURE 4 - CORNER POINT AT INTERSECTION OF S1 AND S2



Unfortunately this "double" normal poses a problem in the finite difference solution where we need to define a relationship between the normal velocity and the potential at P_0 .

To accommodate this we use the following approximation. Let the normal associated with V_0 be shifted to intersect the surface S_1 at a horizontal distance δ_0 and vertical distance, ϵ_0 from the point P_0 . Similarly let the normal associated with V_{0s} intersect S_2 at distances δ_1 and ϵ_0 (see Figure 6). Now for δ_0/α_0 , δ_1/α_1 and ϵ_0/β_0 sufficiently small we can still assume the normals intersect at P_0 thereby facilitating the numerical integration. On the other hand for the shifted positions it is possible to formulate well defined boundary conditions thereby solving the finite difference problem.

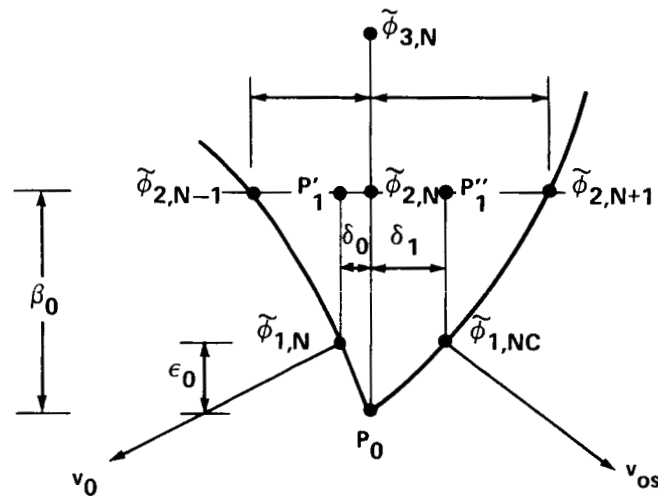


FIGURE 5 - SHIFTED NORMALS AT CORNER POINT P_0



These are ,

$$V_0 = -\cos \Omega_0 \left\{ \frac{\tilde{\phi}_{1,NC} - \tilde{\phi}_{1,N}}{\delta_0 + \delta_1} \right\} - \sin \Omega_0 \left\{ \frac{1 - \frac{\delta_0}{\alpha_0} \tilde{\phi}_{2,N} + \frac{\delta_0}{\alpha_0} \tilde{\phi}_{2,N-1} - \tilde{\phi}_{1,N}}{\beta_0 - \epsilon} \right\} \quad (25)$$

and

$$V_{0s} = \cos \Omega_{0s} \left\{ \frac{\tilde{\phi}_{1,NC} - \tilde{\phi}_{1,N}}{\delta_0 + \delta_1} \right\} - \sin \Omega_{0s} \left\{ \frac{1 - \frac{\delta_1}{\alpha_1} \tilde{\phi}_{2,N} + \frac{\delta_1}{\alpha_1} \tilde{\phi}_{2,N+1} - \tilde{\phi}_{1,NC}}{\beta_0 - \epsilon} \right\} \quad (26)$$

where we have made a linear interpolation to obtain the value of the potential at points P_1' and P_1'' . Note that due to the shifting procedure the equation for the adjacent interior point P_1 will be modified to

$$\begin{aligned} & \frac{-(1+\epsilon_0/\beta_0)}{\beta_0(\beta_0+\beta_1)} \tilde{\phi}_{1,N} + \left\{ \frac{-1}{\alpha_1+\alpha_0} \left(\frac{1}{\alpha_0} - \frac{1}{2\lambda} \right) + \frac{(\epsilon_0/\beta_0)}{\beta_0(\beta_0+\beta_1)} \right\} \tilde{\phi}_{2,N-1} \\ & + \frac{-1}{\beta_1(\beta_0+\beta_1)} \tilde{\phi}_{3,N} + \frac{-1}{(\alpha_1+\alpha_0)} \left\{ \frac{1}{\alpha_0} + \frac{1}{2\lambda} \right\} \tilde{\phi}_{2,N+1} \\ & + \left(\frac{1}{\alpha_1\alpha_0} + \frac{1}{\beta_0\beta_1} \right) \tilde{\phi}_{2,N} = 0 \quad . \end{aligned} \quad (27)$$

This completes the formulation of the finite difference equations.



Solution for the Q Matrix

Combining the equations (18, 20, 24-27, A1-A3) for the interior, axis, and boundary points for ϕ we find

$$[A_{ij}]\{\phi_j\} = R\{v_j\} \quad (i, j = 1, NT) \quad (28)$$

where A_{ij} is a known coefficient matrix, $\{\phi_j\}$ is column vector of the potential values at each of the grid points (NT of them), and $\{v_j\}$ is a column vector of normal velocities or zeros (depending upon whether j indicates a boundary point or an interior point).

Premultiplying (34) by $[A_{ij}]^{-1}$, we find

$$\{\phi_i\} = R[A_{ij}]^{-1}\{v_j\} \quad (29)$$

Picking only those values of i which correspond to boundary points we find the reduced system

$$\{\phi_i\}^b = R[A_{ij}]^{-1}\{v_j\}^b, \quad (30)$$

where $R[A_{ij}]^{-1}$ corresponds to the required Q_{ij} matrix.

From the Q matrix the normal matrix can now be computed as explained in section 3. This concludes the theoretical development for the liquid mass matrix.



5. NUMERICAL RESULTS

A computer program, CTANK1, was written to compute the liquid mass matrix for a cylindrical tank of the type shown in Figure 1. A flow chart and description of this program are given in Appendix B.

Sample Problem

Using this program the liquid mass matrix has been found for the following configuration (see Figure 1):

Cylinder radius = 10 in.

Lower Bulkhead (S2) = 10 in. rad. (spherical)

Invented Bulkhead (S3) = 10 in. rad. (spherical)

Upper Bulkhead (S4) = 10 in. rad. (spherical)

Distance 02 - 01 \triangleq Z02 = 5.8 in.

Distance 04 - 01 \triangleq Z04 = 15.0 in.

Liquid level above 01 \triangleq h01 = 15.3 in.

Liquid density = 0.000376 lbf = sec²/in⁴.

The finite difference grid has been laid out as shown in Figure 1 resulting in fifteen boundary points on the tank surface. Using vertical (Z) and radial (R) degrees-of-freedom this results in 22 degrees of freedom for the liquid mass matrix. The mass matrix is shown in Table 1 (Z and R mass). The ordering of the degrees-of-freedom are Z₁, Z₂, R₂, Z₃, R₃, ..., R₇, R₈, R₉, R₁₀, R₁₁, ..., R₁₄, R₁₅.

TABLE 1 - MATHEMATIC ZEROMASS

[illegible]



Validity of Results

To examine the validity of the derived mass matrix it is normal to first generate a stiffness matrix for the tank containing the liquid and then to use this, together with the mass matrix, to determine the natural frequencies of the liquid-tank system. These natural frequencies are then compared to theoretically or experimentally obtained natural frequencies thereby providing a check for the mass matrix. In the absence of any such results for tanks of the geometry considered here some alternate checks had to be made.

Since from (15),

$$M = \rho/2 [\bar{G}Q + [\bar{G}Q]^T]$$

the correctness of the matrices \bar{G} and Q imply the correctness of the liquid matrix, M . The method for checking the integration matrix, \bar{G} is straightforward and will not be discussed here. The matrix Q (or equivalently $[A_{ij}]^{-1}$) was checked in the following way.

A solution to Laplace's equation (17) subject to the boundary condition $\phi = 0$ on $z = 15.3$ (i.e., $z = 1.53$) is

$$\underline{\phi(\lambda, z) = J_0(\lambda) \sinh(z - 1.53) .} \quad (31)$$

From (31) we find the normal derivative to be

$$\frac{\partial \phi}{\partial n} = J_1(\lambda) \sinh(z - 1.53) \cos \Omega_0 - J_0(\lambda) \cosh(z - 1.53) \sin \Omega_0 \quad (32)$$

where as before Ω_0 is the angle of the outward normal with the horizontal (λ) direction. Now at each of the boundary points we



can compute from (31) the value of the potential $\tilde{\phi}_{Th}$ where the subscript 'Th' indicates the theoretical value of $\tilde{\phi}$.

From (32) we compute the value of $\frac{\partial \tilde{\phi}}{\partial n}$ at each of the boundary points. (Note that they are two values associated with the corner point P_7 .)

Now using (21) in (30) we find

$$\{\tilde{\phi}_i\} = [A_{ij}^{-1}]^b \frac{\partial \tilde{\phi}}{\partial n}_j \quad (i, j = 1, N+1)$$

so from the boundary point values of $(\frac{\partial \tilde{\phi}}{\partial n})$ we find a set of boundary point values for $\tilde{\phi}$. The deviation of these values from $\tilde{\phi}_{Th}$ is a measure of the accuracy of the $[A_{ij}^{-1}]^b$ and Q_{ij} matrices. For the sample problem solved here the values are shown in Table 2. It is seen that the maximum error is 4.4%, which reduces to approximately 2.6% as one leaves the neighborhood of the corner point. Bearing in mind the coarseness of the finite difference grid this shows the $[A_{ij}^{-1}]^b$ is being correctly determined.

The second check that was made is a global check for the mass matrix and consists of using the Matrix M to find the total weight of the liquid. For the sample problem it was found:

Total weight (theoretical) = 1.0 units,
Total weight (computed from M) = 0.9956 units,
Percent error = 0.44%.



| Point | ϕ_{Th} | ϕ_{Comp} | % Error |
|-----------------|-------------|---------------|---------|
| P ₁ | - .5552 | - .5698 | 2.64 |
| P ₂ | - .5724 | - .5807 | 1.44 |
| P ₃ | - .6409 | - .6541 | 2.04 |
| P ₄ | - .7699 | - .7937 | 3.10 |
| P ₅ | - .9245 | - .9587 | 3.70 |
| P ₆ | -1.0555 | -1.0965 | 3.88 |
| P ₇ | -1.2409 | -1.2955 | 4.40 |
| P ₇ | -1.2409 | -1.2944 | 4.31 |
| P ₈ | -1.0016 | -1.0428 | 4.11 |
| P ₉ | - .8413 | - .8755 | 4.07 |
| P ₁₀ | - .6592 | - .6851 | 3.92 |
| P ₁₁ | - .5146 | - .5335 | 3.66 |
| P ₁₂ | - .4424 | - .4573 | 3.37 |
| P ₁₃ | - .4248 | - .4387 | 3.28 |
| P ₁₄ | - .2815 | - .2895 | 2.86 |
| P ₁₅ | - .1385 | - .1421 | 2.64 |

Table 2 - LOCAL ERROR IN $[A^{-1}]^b$ MATRIX



Comparison with "Statical" Mass Matrix

The configuration for the sample problem was chosen so that the total mass of the liquid was unity. This enables the reader to see from Table 1 how the mass is distributed to the degrees-of-freedom. In particular it is interesting to compare the distribution with that obtained from a "statical" analysis. (In such an analysis the mass associated with a given degree of freedom is derived from the weight of the column of liquid above the corresponding node point.)

For the statical mass matrix the only non zero terms are

$$\begin{aligned}(Z1, Z1) &= .630 - 02 (.236 - 02) \\(Z2, Z2) &= .740 - 01 (.153 - 01) \\(Z3, Z3) &= .159 + 00 (.480 - 01) \\(Z4, Z4) &= .236 + 00 (.689 - 01) \\(Z5, Z5) &= .211 + 00 (.497 - 01) \\(Z6, Z6) &= .152 + 00 (.377 - 01) \\(Z7, Z7) &= .990 - 01 (.316 - 01) \\(Z8, Z8) &= .350 - 01 (.320 - 02)\end{aligned}$$

where the corresponding terms for the hydroelastic matrix are shown in parenthesis. It is seen that the "statical" masses are consistently higher than those obtained from the hydroelastic analysis. Furthermore the statical matrix lacks any components associated with the radial degrees-of-freedom and any coupling between the degrees-of-freedom which, for a liquid representation is a serious defect.

6. CONCLUSIONS

In this memorandum a procedure is described for finding the mass matrix of an incompressible, inviscid liquid contained in a cylindrical tank with an inverted lower bulk-head. A computer program, CTANK1., has been written which on input of the tank dimensions, the liquid density and a consistent set of boundary point locations, can be used to compute this mass matrix.

A sample problem has been solved using this program, and two theoretical checks carried out on the computed mass matrix. These checks showed the accuracy of the numerical method to be very good. Furthermore, the program has been



used to derive mass matrices for the S-IVB LH₂ at various flight times. When these matrices were incorporated into an overall structural model of the S-IVB and a vibration analysis carried out, the predicted structural response correlated well with flight data. This work will be described in a forthcoming report.

ACKNOWLEDGEMENT

I wish to thank M. L. Carothers for valuable assistance with the computer programming.

A handwritten signature in black ink, appearing to read 'T. J. Rudd', written in a cursive style.

T. J. Rudd

2031-TJR-jf

Attachments
References
Appendices A and B



REFERENCES

1. Guyan, R. J., Ujihara, B. H. and Welch, P. W., "Hydroelastic Analysis of Axisymmetric Systems by a Finite Element Method", AFFDL-TR-68-150, Proceedings of the Second Conference on Matrix Methods in Structural Mechanics, December 1969.
2. Goldman, R. L., "Longitudinal Vibration Analysis of Partially-Filled Ellipsoidal Tanks by Finite Differences", TR-70-6C RIAS, August 1970.
3. Rudd, T. J., "On the Calculation of the Pressure Fluctuation in a Vibrating Propellant Tank", Bellcomm Memorandum for File, B71 03052, March 23, 1971.
4. Vandergraft, J. S., "A Finite Difference Method for Solving Laplace's Equation Using a Non-Uniform Mesh", Bellcomm Technical Memorandum, TM-71-2031-1, March 23, 1971.



APPENDIX A

In this appendix the equations for boundary points on the surfaces S2, S3 and S4 are given.

Boundary Point on S2

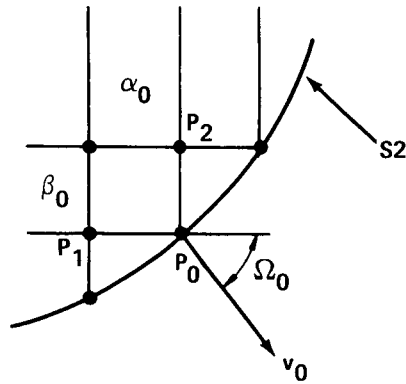


FIGURE A1 - BOUNDARY POINT ON S2

$$-\frac{\cos \Omega_0}{\alpha_0} \phi(P_1) - \frac{\sin \Omega_0}{\beta_0} \phi(P_2) + \left(\frac{\cos \Omega_0}{\alpha_0} + \frac{\sin \Omega_0}{\beta_0} \right) \phi(P_0) = Rv_0 \quad . \quad (A1)$$



Boundary Point on S3

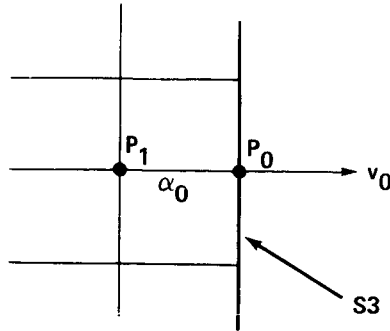


FIGURE A2 - BOUNDARY POINT ON S3

$$-\frac{\cos \Omega_0}{\alpha_0} \tilde{\phi}(P_1) - \frac{\sin \Omega_0}{\beta_0} \tilde{\phi}(P_2) + \left(\frac{\cos \Omega_0}{\alpha_0} + \frac{\sin \Omega_0}{\beta_0} \right) \tilde{\phi}(P_0) = Rv_0 . \quad (A2)$$

Boundary Point on S4

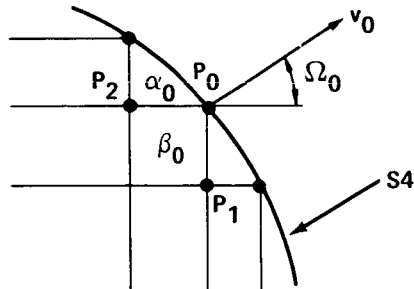


FIGURE A3 - BOUNDARY POINT ON S4

$$-\frac{\cos \Omega_0}{\alpha_0} \tilde{\phi}(P_1) - \frac{\sin \Omega_0}{\beta_0} \tilde{\phi}(P_2) + \left(\frac{\cos \Omega_0}{\alpha_0} + \frac{\sin \Omega_0}{\beta_0} \right) \tilde{\phi}(P_0) = Rv_0 . \quad (A3)$$



APPENDIX B

In this appendix the computer program CTANK1., which is suitable for use with the UNIVAC 1108, is described. Here we will restrict the description to the basic version of CTANK1. which is suitable for configurations where the liquid level is below the start of the upper bulkhead S4. Furthermore, it is restricted to those configurations where the total number of grid points is less than 200. (See Note 1 on page B2).

A flow chart showing the main operations in the program is shown in Figure B1. The input is in two parts as follows:

\$FIRST

N = Number of boundary points on S1.

NT = Number of boundary points on S2 including the intersection points with S1 and S3.

NS = Number of boundary points on S3 excluding the intersection point on S2 and the free surface.

IP = Print parameter: If = 1, A and A^{-1} are printed.
If = 0 only those items shown in flow chart.

\$END

\$INPUT

ZEE = Single array, of size $(N+NT-1+NS)$, of boundary point heights above the origin O1. The array begins with the points on S1 (starting from lowest) followed by the points on S2 and S3 (starting with the lowest but excluding the corner point).

Z02 = Distance of the origin O2 above O1.

A1,B1 = Semi-major and minor axes of the ellipse containing S1

A2,B2 = Semi-major and minor axes of the ellipse containing S2.

WL = Density of liquid propellant.

\$END.



As an example, the input for the sample problem discussed in section 5 is as follows:

\$FIRST

N = 7, NT = 3, NS = 2, IP = 0 ,

\$END

\$INPUT

ZEE(1) = 2.9, 4.5, 5.8, 7.5, 9.0, 9.8, 10.0, 4.5, 5.8,
7.5, 9.0, 9.8, 10.0, 11.7, 13.5, 15.3,

Z ϕ 2 = 5.8, A1 = 10.0, B1 = 10.0, A2 = 10.0, B2 = 10.0,

WL = 0.000376,

\$END.

NOTE 1.

The total number of grid points is given by

$$N_{\text{Total}} = (NT^2 + 1) + \frac{(N - NT)}{2} \{N + 3NT - 1\} + NS (NT + N - 1)$$

For the basic version of CTANK1., N_{Total} must not exceed 200.

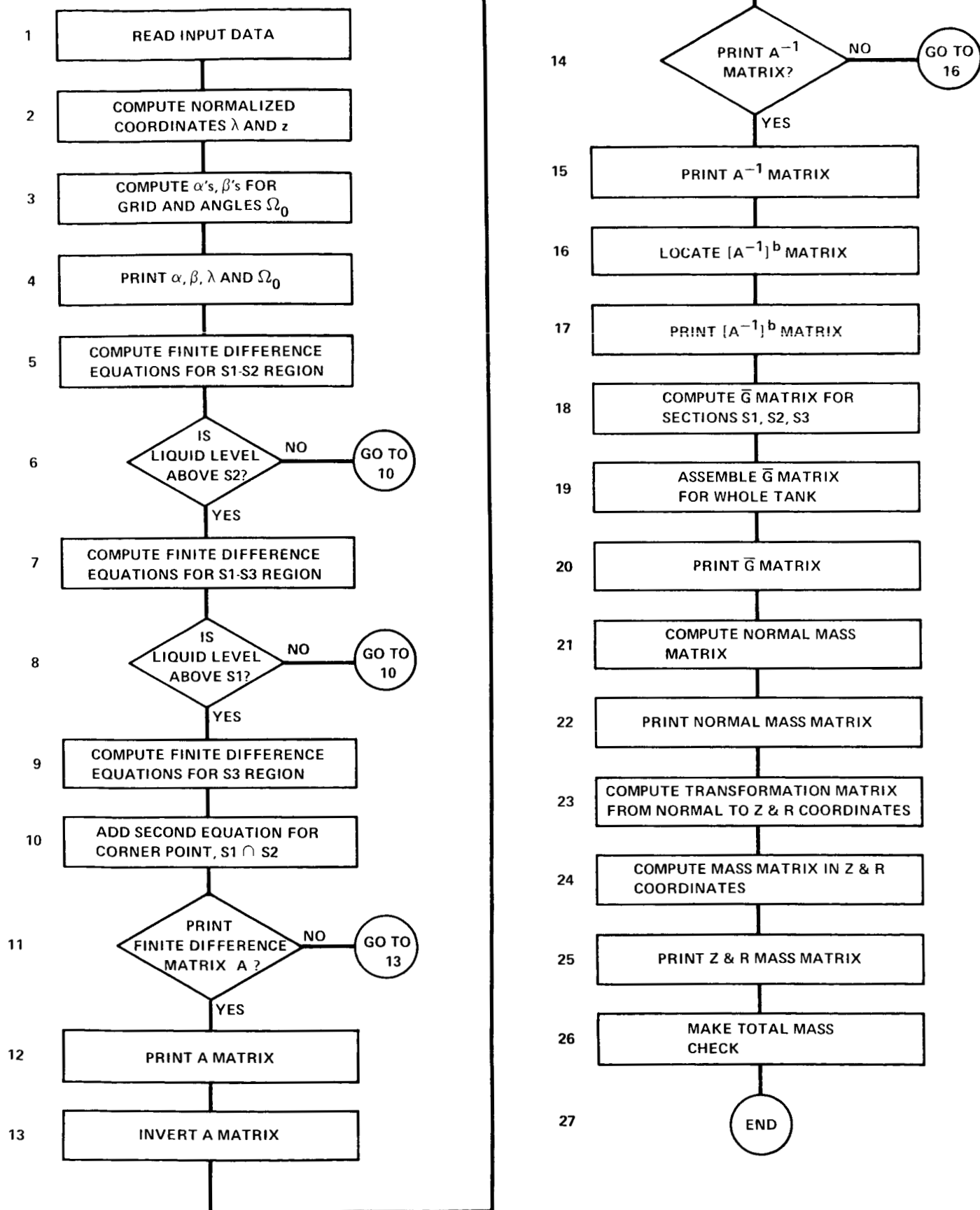


FIGURE B1 - FLOW CHART FOR BASIC VERSION OF CTANK1



Subject: A Hydroelastic Model for a Cylindrical
Tank with an Inverted Bulkhead - Case 320

From: T. J. Rudd

Distribution List

NASA Headquarters

A. S. Lyman/MAP (2)
W. E. Stoney/MAE

MSFC

T. Bullock/S&E-ASTN-ADL
L. A. Kiefling/S&E-ASTN-DDS
L. B. Mulloy/S&E-ASTN-A
J. B. Sterett/S&E-ASTN-A

MSC

D. C. Wade/FS2

Lockheed

C. W. Coale

North American

R. Schwartz
B. H. Ujihara
H. Weiner

Aerospace Corp.

S. Rubin

Boeing, Huntsville

J. E. Kennedy
L. D. McTigue
G. F. Riley

RIAS

R. L. Goldman

University of Maryland

J. S. Vandergraft

Bellcomm

G. M. Anderson
A. P. Boysen, Jr.
J. P. Downs*
D. R. Hagner
J. J. Hibbert
W. W. Hough
J. Z. Menard
I. M. Ross*
P. F. Sennewald
J. W. Timko*
R. L. Wagner
M. P. Wilson*

All Members of Department 2031
Central File
Department 1024 File
Library

*Abstract Only